Dynamic modelling and open-loop control of a twin rotor multi-input multi-output system

S M Ahmad[1], A J Chipperfield[2] and M O Tokhi[2]*
[1]Department of Mechanical and Marine Engineering, University of Plymouth, UK
[2]Department of Automatic Control and Systems Engineering, University of Sheffield, UK

Abstract: A dynamic model for a one-degree-of-freedom (DOF) twin rotor multi-input multi-output (MIMO) system (TRMS) in hover is obtained using a black-box system identification technique. The behaviour of the TRMS in certain aspects resembles that of a helicopter; hence, it is an interesting identification and control problem. This paper investigates modelling and open-loop control of the longitudinal axis alone, while the lateral axis movement is physically constrained. It is argued that some aspects of the modelling approach presented are suitable for a class of new generation or innovative air vehicles with complex dynamics. The extracted model is employed for designing and implementing a feedforward/open-loop control. Open-loop control is often the preliminary step for development of more complex feedback control laws. Open-loop control strategies using shaped command inputs are accordingly investigated for resonance suppression in the TRMS. Digital low-pass and band-stop filter shaped inputs are used on the TRMS testbed, based on the identified vibrational modes. A comparative performance study is carried out and the corresponding results presented. The low-pass filter is shown to result in better vibration reduction.

Keywords: helicopter, system identification, twin rotor MIMO system, open-loop control, vibration suppression

NOTATION

a_i, b_i, c_i	unknown parameters to be identified
ARMAX	auto-regressive moving average with exogenous input model
d.c.	direct current
$e(t)$	zero mean white noise
E	expected or mean value
f	frequency (Hz)
F1, F2	thrust generated by the rotors in the vertical and horizontal planes respectively
na, nb, nc	orders of the A, B and C polynomials of the ARMAX model
S_{xx}, S_{yy}	auto power spectral densities of input and output signals respectively
S_{xy}	cross-spectral density between a pair of input and output signals
TRMS	twin rotor multi-input multi-output system
$u_1(t)$	input to the main rotor (V)
$y_1(t)$	pitch angle (rad)
$\gamma_{xy}^2(f)$	ordinary coherance function
$\varepsilon(t)$	prediction errors or residuals

The MS was received on 22 August 2001 and was accepted after revision for publication on 18 February 2002.
* *Corresponding author: Department of Automatic Control and Systems Engineering, University of Sheffield, Mappin Street, Sheffield S1 3JD, UK.*

1 INTRODUCTION

The development of a 6 degree-of-freedom (DOF) model for a conventional aircraft/helicopter from first principles is well established. The underlying assumption in the formulation of these models is that the vehicle is regarded as a rigid body; i.e. no structural deformation of the vehicle body occurs. These models can therefore accurately describe the vehicle dynamics in the low-frequency range. However, with the advent of lightweight flexible material and its increasing use in aerospace applications such as fighter aircraft [**1**], missiles [**2**] and helicopters [**3**], the need to account for aeroelastic effects will make modelling very crucial for such vehicles. Air vehicles possessing some degree of flexibility clearly cannot be modelled by the rigid-body assumption alone. For instance, Waszak and Schmidt [**4**] demonstrated the importance of modelling aeroelastic dynamics for a high-speed transport aircraft with a moderate level of structural flexibility. Neglecting the aeroelastic dynamics in the model resulted in a model that erroneously indicated the aircraft to have a stable phugoid mode and had errors in short period frequency and damping of approximately 55 and 14 per cent respectively, compared to the complete aeroelastic aircraft model. Therefore, for flexible systems it is imperative to resort to modelling techniques that incorporate rigid-body degrees of freedom as well as elastic degrees of freedom in a unified manner. Further, with the introduction of many innovative aircraft designs such as tilt wing, delta wing or canard control surfaces, X wing and tilt body, the modelling challenge has also increased many fold.

To model classical and innovative air vehicles, including the flexible one, the following approaches can be potentially employed:

1. Mathematical models. This approach describes the vehicle dynamics by a set of differential equations relating the external forces and moments in terms of acceleration, state and control variables, where the parameters are the stability and control derivatives. For a flexible aircraft there are additional terms for elastic stability derivatives [**5**]. The fidelity of these models is then improved iteratively by comparing the model and aircraft responses and employing suitable parameter identification methods. In essence, the role of a system identification method is to estimate physically defined aerodynamic and flight mechanics parameters from flight or wind tunnel data. A good account of parametric system identification for flight applications can be found in references [**6**] and [**7**] and references therein. Lately, a modelling approach based on frequency domain system identification has been developed and successfully applied to both full-scale and laboratory helicopters [**8–10**].
2. Black-box models. The physics-based modelling approach requires considerable knowledge about vehicle dynamics in order to obtain the governing equations. An alternative is to adopt black-box system identification, which is an experimental technique and has proved to be an excellent tool to model complex processes where it is not always possible to obtain reasonable models using physical insight alone (e.g. innovative aircraft that are inherently more complex than their conventional counterpart). This method enables the engineer to identify the key flight dynamic characteristics of the vehicle and therefore allows the analyst to focus on the modelling effort of these characteristics. The modelling is done assuming no prior knowledge of model structure, order or parameters relating to physical phenomena, i.e. black-box modelling. Such an approach yields input–output transfer function models with neither prior-defined model order nor specific parameter settings reflecting any physical aspects. It is then the responsibility of the systems engineer to examine the resultant black-box model and interpret the identified model order and estimated parameters in relation to the plant dynamics.
3. Grey-box models. This approach can be employed when some physical insight is available, but several parameters remain to be determined from flight or wind tunnel data.

This work addresses modelling of an experimental test-rig, representing a complex twin rotor multi-input multi-output (MIMO) system (TRMS), shown in Fig. 1. In addition to the rigid-body dynamics, the TRMS also exhibits elastic motion, thereby increasing the modelling complexity. Further details about the TRMS are given in Sections 2 and 3. In view of the complexities involved, the modelling problem is analysed and solved using the first two approaches, i.e. (a) the physics-based approach and (b) the black-box approach. The physics of the

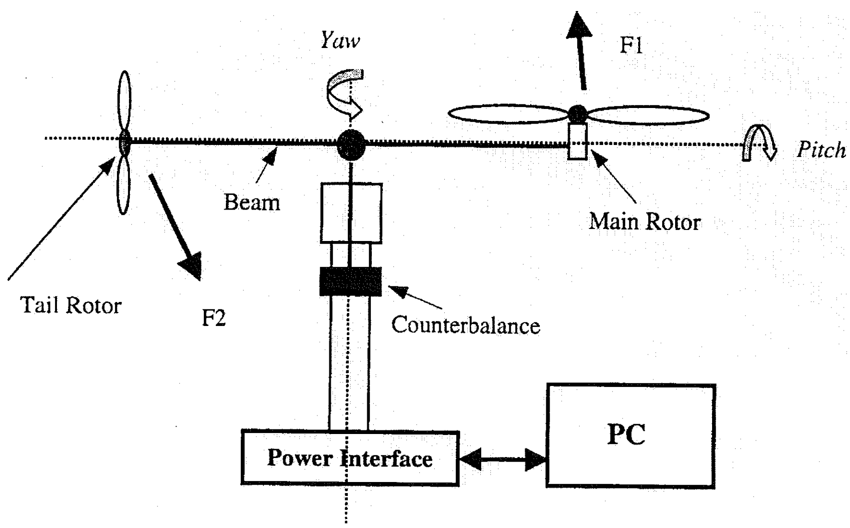

Fig. 1 The twin rotor MIMO system

TRMS is implicity used, albeit in a sense that two states are required to describe each rigid-body motion; i.e. a second-order differential equation is all that is required to describe the 1 DOF motion. If only rigid-body dynamics were to be modelled, then the only other major problem would have been to find the coefficients of the differential equation by either examining the physical properties of the material or through system identification. Since the TRMS also undergoes structural deformation, a second-order system description would be inaccurate, as there is every likelihood that dynamic flexible effects would influence the 'rigid-body' system response. This work therefore first utilizes the spectral method to identify key system modes and then the black-box system identification technique to arrive at a reasonable TRMS model. This work is an extension of the authors' previous paper [**11**].

In this paper, attention is first focused on the identification and verification of longitudinal dynamics of a 1 DOF TRMS with its main beam (body) in a flat horizontal position representing the hover mode. Although the system permits multi-input multi-output (MIMO) experiments, only a single-input single-output (SISO) set-up will be discussed. The authors' work on 2 DOF MIMO modelling is reported in reference [**12**].

In the latter part of the paper the issue of detection and attenuation of vibrational modes is discussed. This is based on the SISO modelling approach presented in the first part of the paper. A feedforward control technique, which is related to a number of approaches known as 'input shaping control', is investigated. In these methodologies, a feedforward input signal is shaped so that it does not contain spectral components at the system's resonance eigenfrequencies. The approach requires the natural resonance frequencies of the system to be determined through suitable identification and modelling techniques. The input command shaping technique is widely employed in flexible aircraft [**1**] and helicopter control [**13**]. Investigation of open-loop control is a prelude to a future study of the development of more complex feedback control laws. The paper is organized as follows. Section 2 provides the motivation for this work. Section 3 gives a description of the experimental set-up. Section 4 deals with identification experiments and Section 5 presents the results. Section 6 delves into vibration mode analysis and control. Section 7 discusses filter design and implementation and Section 8 concludes the paper.

2 MOTIVATION

Although the twin rotor MIMO system (TRMS) shown in Fig. 1 does not fly, it has a striking similarity to a helicopter, such as system non-linearities and cross-coupled modes. The TRMS can therefore be perceived as an unconventional and complex 'air vehicle' with a flexible main body. These system characteristics present formidable challenges in modelling, control design and analysis. The TRMS is a laboratory set-up designed for control experiments by Feedback Instruments Limited [**14**]. The main differences between the helicopter and the TRMS are as follows:

1. In a single main rotor helicopter the pivot point is located at the main rotor head, whereas in the case of the TRMS the pivot point is midway between the two rotors.
2. In a helicopter, lift is generated via collective pitch control, i.e. pitch angles of all the blades of the main rotor are changed by an identical amount at every point in the azimuth, but at the constant rotor speed. However, in the case of the TRMS, pitch angles of all the blades are fixed and speed control of the main rotor is employed to achieve vertical control.
3. Similarly, yaw is controlled in a helicopter by changing, by the same amount, the pitch angle of all the blades of the tail rotor. In the TRMS, yawing is affected when the tail rotor speed is varied.
4. There are no cyclical controls in the TRMS; cyclic is used for directional control in a helicopter.

However, like a helicopter there is a strong cross-coupling between the collective (main rotor) and the tail rotor.

Although the TRMS rig reference point is fixed, it still resembles a helicopter, by being highly non-linear with strongly coupled modes. Such a plant is thus a good benchmark problem to test and explore modern identification and control methodologies. The experimental set-up simulates similar problems and challenges encountered in real systems. These include complex dynamics leading to both parametric and dynamic uncertainty, unmeasurable states, sensor and actuator noise, saturation and quantization, bandwidth limitations and delays.

The presence of flexible dynamics in the TRMS is an additional motivating factor for this research. There is an immense interest in design, development, modelling and control of flexible systems, due to its utility in a multitude of applications, e.g. in aerospace and robotics.

3 THE TRMS SYSTEM

The TRMS considered in this work is described in Fig. 1. This consists of a beam pivoted on its base in such a way that it can rotate freely both in its horizontal and vertical planes. There are rotors (the main and tail rotors), driven by d.c. motors, at both ends of the beam. A counterbalance arm with a weight at its end is fixed to the beam at the pivot. The state of the beam is described by four process variables: yaw and pitch angles measured by position sensors fitted at the pivot and two corresponding angular velocities. Two additional state variables are the angular velocities of the rotors, measured by tachogenerators coupled with the driving d.c. motors.

In a typical helicopter, the aerodynamic force is controlled by changing the angle of attack of the blades. The laboratory set-up is constructed such that the angle of attack of its blades is fixed. The aerodynamic force is controlled by varying the speed of the motors. Therefore, the control inputs are supply voltages of the d.c. motors. A change in the voltage value results in a change of the rotational speed of the propeller, which results in a change of the corresponding angle (in radians) of the beam [**14**], F1 and F2 in Fig. 1 represent the thrust generated by the rotors in the vertical and horizontal planes respectively.

4 PRELIMINARY EXPERIMENTATION

The objective of the identification experiments is to estimate a linear time-invariant (LTI) model of the 1 DOF TRMS in hover without any prior system knowledge pertaining to the exact mathematical model order or structure. No model order is assumed *a priori*, unlike aircraft system identification wherein the identification procedure is reduced to estimating the coefficients of a set of differential equations describing the aircraft dynamics. The differential equations describe the external forces and moments in terms of accelerations, state and control variables, where the coefficients are the stability and control derivatives.

The extracted model is to be utilized for low-frequency vibration control and design of a suitable feedback control law for disturbance rejection and reference tracking. Hence, accurate identification of the rigid-body dynamics is imperative. This would also facilitate understanding of the dominant modes of the TRMS. Since no mathematical model is available, a level of confidence has to be established in the identified model through rigorous frequency and time-domain analyses and cross-validation tests.

It is intuitively assumed that the body resonance modes of the TRMS lie in the low-frequency range of 0–3 Hz, while the main rotor dynamics are at significantly higher frequencies. The rig configuration is such that it permits open-loop system identification, unlike a helicopter, which is open-loop unstable in hover mode. During experimentation, the yaw plane movement is physically locked, thereby allowing only pitch plane motion, i.e. only thrust F1 is active and since the yaw plane is locked, F2 (tail rotor) does not have any influence in this plane.

4.1 Flight test data

The TRMS has been upgraded, and a joystick control analogous to that of a helicopter pilot stick has been provided. Test signals could be applied using the stick. However, only a very simple signal sequence is feasible, which is not sufficient for adequacy of spectral content and repeatability. Moreover,the system is very sensitive and precise control cannot be exercised. Hence, the test signal is designed separately and read from the workspace in the MATLAB SIMULINK environment, instead of using the stick. This is analogous to automation of the test signal, which ensures that the experiments are sufficiently controlled and repeatable, and guarantees the desired spectral content.

The trim configuration was in a steady state horizontal position of the boom of the TRMS (see Fig. 2). Since the TRMS is very sensitive to atmospheric disturbances, the tests were conducted in practically calm air. The system was excited with pseudo random binary sequence (PRBS) signals of different bandwidths (2–20 Hz) in order to ensure that all resonance modes are captured in the range of interest, i.e. 0–3 Hz, and out of curiosity to find out whether any modes exist beyond this range. Finally, a PRBS of 5 Hz bandwidth and duration of 60 s was deemed fit for this study. The PRBS is shown in Fig. 3a. The PRBS magnitude was selected so that it does not drive the TRMS out of its linear operating range. Good excitation was achieved from 0 to 2.5 Hz, which includes all the important rigid-body and flexible modes (see Fig. 3b). It is noted that the significant system modes lie in the 0–1 Hz bandwidth.

4.2 Data reliability analysis

Measurements used for system identification were pitch angle y_1 in radians and control u_1 in volts. The measured data were sampled and recorded on a PC using real-time kernel (RTK) software. Data quality and consistency are critical to the identification. Excessively noisy or kinematically inconsistent data may lead to identification of an incorrect model. Preliminary checks of data quality and consistency can ensure that these sources of error are minimized. The TRMS is very sensitive to the atmospheric disturbances and in order to ensure accurate identification each signal was repeated many times until a response, undisturbed by a gust of air, was obtained. This was ensured by operating the system in a gust-free environment.

4.2.1 Sampling rate

One of the important considerations in discrete-time systems is the sampling rate. A low sampling rate would yield data with little information about the process dynamics. A high sampling rate, on the other hand, will lead to a poor signal-to-noise ratio (SNR). A low SNR means less informative data and the estimation would be biased. A good choice of sampling rate is thus a tradeoff between noise reduction and relevance for the process dynamics.

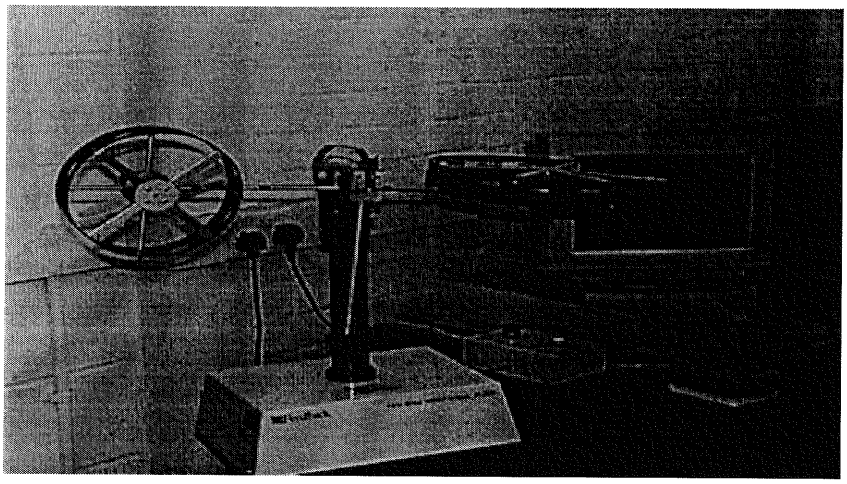

Fig. 2 The TRMS in operational mode

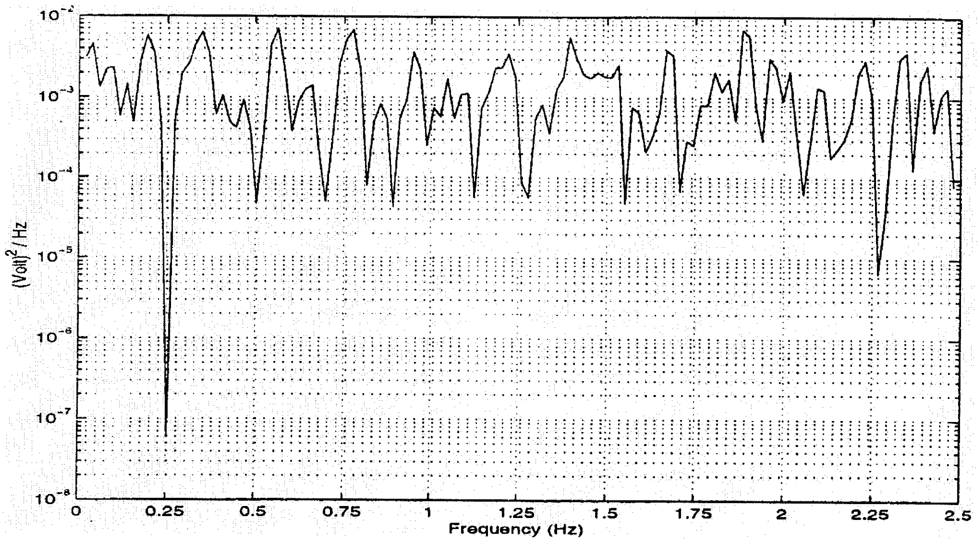

(a) PRBS

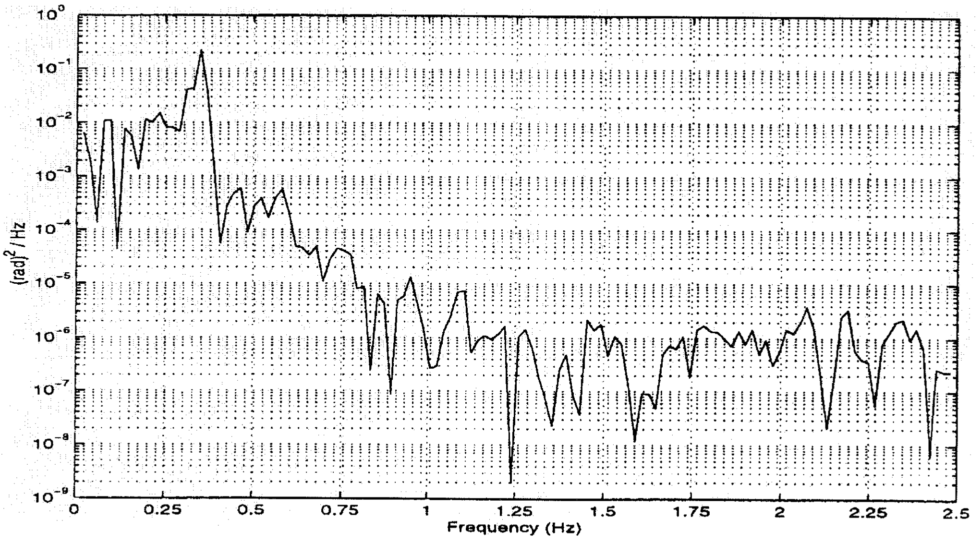

(b) Pitch response

Fig. 3 Power spectral density

Since the intended use of the system model is for control purposes, certain other aspects need to be considered. It is recommended that the sampling interval for which the model is built should be the same for the control application [15]. There are, however, some useful guidelines, which relate the sample interval to the response of the system to be identified. Certain symptoms will appear in the estimated model if a wrong sample interval is selected. This can be done by observing the positions of the poles of the obtained model in the z plane. If the poles and zeros are found clustered tightly around $|z| = 1$, this indicates that the system has been sampled too rapidly. If the poles and zeros are found clustered tightly around the origin of the z plane, this indicates that the system has been sampled too slowly. The ideal aim is for a set of estimated model parameters that correspond to a reasonable spread of pole-zero positions in the z plane [16].

There are some useful rules of thumb for setting the initial sampling rate, based on the time constant (i.e. from the step response), process settling time and guessed bandwidth of the system. For instance, a sampling rate could be chosen that is (a) one-fifth of the time constant or 10 times the guessed system bandwidth [15], (b) four times the guessed system bandwidth [16] or (c) 10 per cent of the settling time [17], with the optimal choice lying around the time constant of the system. The step response of the plant is given in Fig. 4. It is noted that the dynamics of the system are not simple, with highly oscillatory poles, the dominating time constant is around 1.2 s and there is a pure time delay of about 0.6–0.7 s.

Using the above guidelines a sampling rate of 5 Hz was chosen iteratively. At this rate only the mildly unstable system poles were close to the unit circle and the rest well within the unit circle (see Fig. 5). Hence a sampling rate of 5 Hz was found to be appropriate for this case study. In retrospect, the sampling rate is close to 10 times the identified system bandwidth (refer to Section 4.1). It can also be deduced from Fig. 5 that the system is inherently non-minimum phase, with zeros outside the unit circle. This is also evidenced in Fig. 4, as the step response undershoots at the start. Note that the pole-zero plot of the identified TRMS model is presented here in order to illustrate the effect of the sampling period. The identified model parameters are presented in Section 5.6.

4.3 Coherence test for linearity

It is important in linear system identification to keep the effects of non-linearities to a minimum. The coherence is a measure of linear dependence of the output on the input, defined in spectral terms; i.e. it expresses the degree of linear correlation in the frequency domain between the input and the output signals. An important use of the coherence spectrum is its application as a test of the signal-to-noise ratio and linearity between one or more input variables and an output variable. The coherence function $\gamma^2_{xy}(f)$ is given by

$$\gamma^2_{xy}(f) = \frac{|S_{xy}(f)|^2}{S_{xx}(f)S_{yy}(f)} \tag{1}$$

where S_{xx} and S_{yy} are the auto-spectral densities of the input and output signals respectively and S_{xy} is the cross-spectral density between the input and output signals. By definition, the coherence function lies between 0 and 1 for all frequencies f:

$$0 \leqslant \gamma^2_{xy}(f) \leqslant 1$$

If $x(t)$ and $y(t)$ are completely unrelated, the coherence function will be zero, while a totally noise-free linear system would yield $\gamma^2_{xy}(f) = 1$. The coherence function

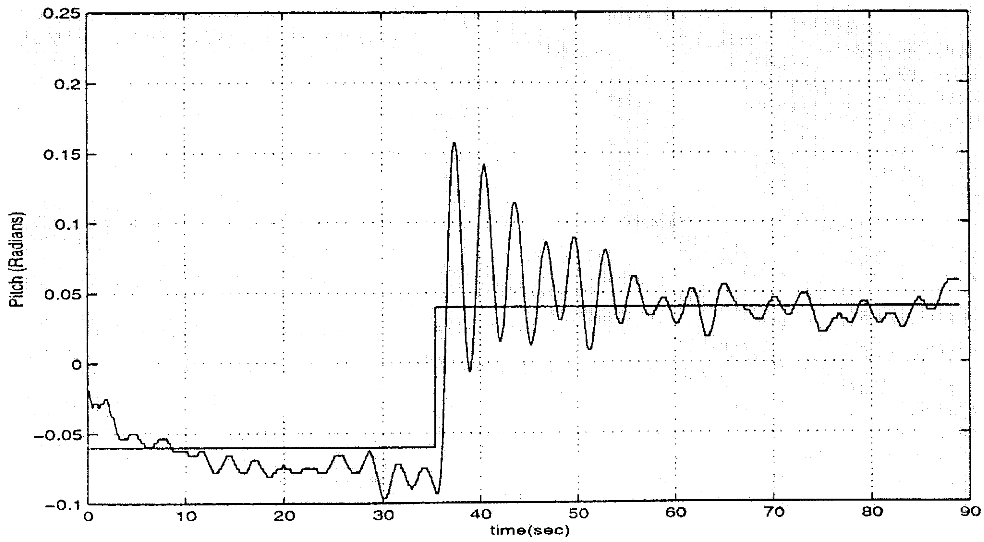

Fig. 4 Step response of the process

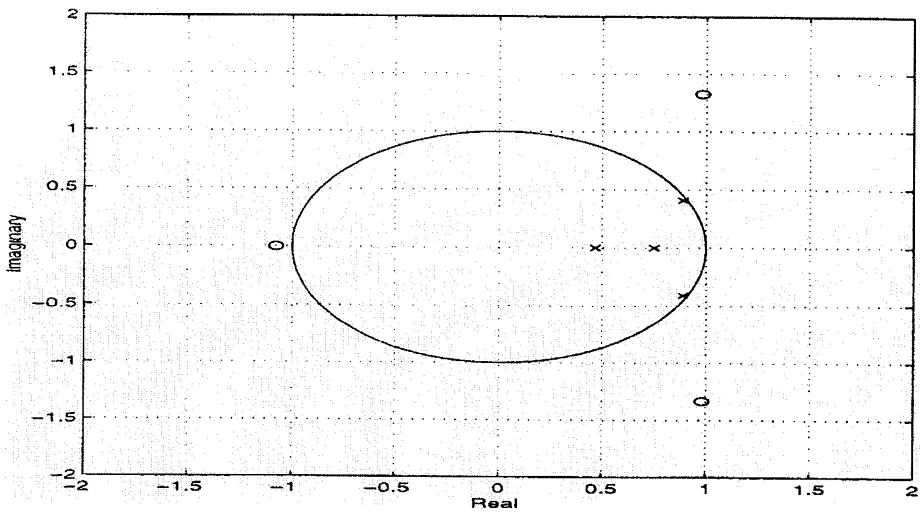

Fig. 5 Pole-zero plot

may thus be viewed as a type of correlation function in the frequency domain where a coherence function not equal to 1 indicates the presence of one or more of the following [**18**]:

1. Extraneous noise is present in the input and the output measurements.
2. The system relating $x(t)$ and $y(t)$ is not linear.
3. The output $y(t)$ is due to an input $x(t)$ as well as other inputs such as external disturbances.
4. Resolution bias errors are present in the spectral estimates.

When a system is noisy or non-linear, the coherence function indicates the accuracy of a linear identification as a function of frequency. The closer it is to unity at a given frequency, the more reliance can be placed on an accompanying frequency-response estimate, at that frequency. For a real application, which will be non-linear and affected, to some extent by noise, a plot of the coherence function against frequency will indicate the way in which the disturbances change across the frequency band. The coherence test is employed on the input–output data channel and is discussed next.

The linearity of the operating region is confirmed by a flat coherence of unity between the input PRBS signal and the output pitch response. Coherence spectra with a 5 Hz sampling rate are shown in Fig. 6a. The poor quality could be due to one or a combination of the four reasons mentioned above. The presence of extraneous noise such as electronic noise or jitters in the input–output measurements is ruled out as the sensors provide direct digital output. Since it is an SISO experiment there is no other input influencing the output. Moreover, care was taken to keep the ambience disturbances to a minimum. Condition 3 above is, therefore, not applicable. Further, the input magnitude was deliberately kept small to prevent a non-linear system response. Therefore, poor quality is most likely due to resolution bias errors. Hence, the input–output data were resampled at a rate of 10 Hz, and the corresponding coherence function is depicted in Fig. 6b. This has an improved resolution, but, as with Fig. 6a, there is a notch in the proximity of 0.4 Hz, which could be due to the non-linear behaviour of the system at that frequency. Figure 6b thus corroborates the linear input–output relationship that is necessary to obtain a reasonable linear model.

It is important to highlight here, that the coherence test has been widely employed in helicopter system identification [**8–10, 19**], mainly to detect cross-coupling effects between various input–output channels and the degree of non-linearity present in the system under test. The authors also successfully employed this technique to identify the cross-coupling effect in 2 DOF TRMS modelling [**12**]. However, since the current paper is confined to 1 DOF modelling, the utility of coherence function is also limited, primarily to establish whether the system behaviour is linear or non-linear.

5 DYNAMIC MODELLING OF THE TRMS

This section discusses the identification of the TRMS, which involves three steps:

1. The first step is qualitative operation, which defines the structure of the system for example, type and order of the differential/difference equation relating the input to the output; it is known as *characterization*. This means selection of a suitable model structure, e.g. auto-regressive with exogenous input (ARX), auto-regressive moving average with exogenous input (ARMAX), Box–Jenkins and model order capable of capturing the system dynamics.
2. The second step is *identification/estimation*. This consists of determining the numerical values of the structural parameters that minimize an error between the

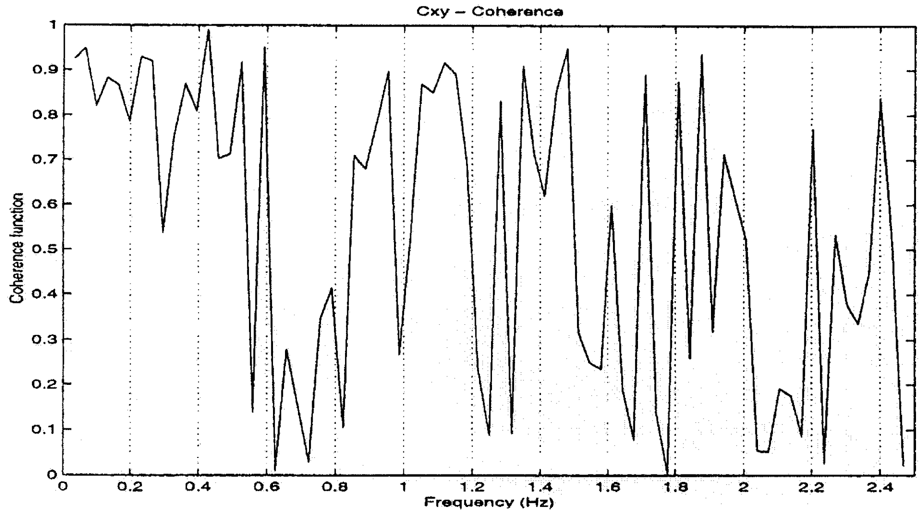

(a) Data sampled at 5 Hz

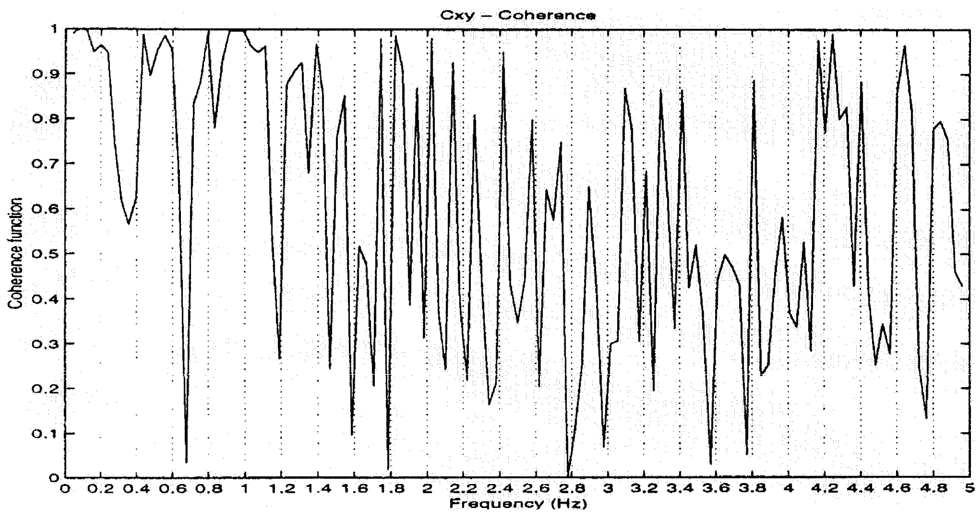

(b) Data sampled at 10 Hz

Fig. 6 Coherence test

system to be identified and its model. Common estimation methods are the least-squares (LS) method, the instrumental variable (IV) method, the maximum-likelihood (MLE) method and the prediction-error method (PEM). This is, in simple terms, a curve-fitting exercise.

3. The third step, *validation*, consists of relating the system to the identified model responses in time or frequency domain to instil confidence in the obtained model. Residual test, bode plots and cross-validation tests are generally employed for model validation.

These main features of system identification are symbolically indicated in Fig. 7. The objective of identification is to minimize the sum-squared errors or residuals $\varepsilon(t)$. More details on the general aspects of identification theory can be found in references [**15**] and [**17**].

5.1 Mode or structure determination

To identify an unknown process, some knowledge or engineering judgement of the process and type of excitation signal is required. The parameters of physical systems are generally distributed in space. Hence, the systems will have more than one frequency of resonance. The primary interest in this work lies in locating these resonances or normal modes, which ultimately dictate the behaviour of the system. Theoretically, the TRMS will have an infinite number of such normal modes with associated frequencies. It is observed from the power spectral density in Fig. 3 that the significant system modes lie in the 0–1 Hz bandwidth, with a main resonance mode at 0.34 Hz, which can be attributed to the main body dynamics. A model order of 2, 4 or 6 corresponds to prominent normal modes at

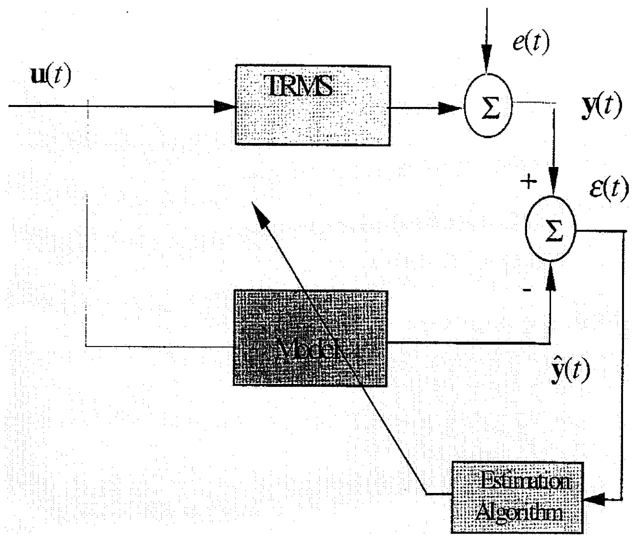

Fig. 7 The identification procedure

0.34 and 0.46 Hz and a rigid-body pitch mode is thus anticipated.

5.2 Parametric modelling

Equipped with the insight mentioned above, attention is focused on employing parameters in the model to obtain the best system description. A parametric method can be characterized as a mapping from the experimental data to the estimated parameter vector. Such models are often required for control application purposes. With no prior knowledge of sensor or instrument noise, a preliminary second-order ARX model was assumed for the $u_1 \rightarrow y_1$ channel. The auto-correlation of residuals revealed negative correlation at lag 1, indicating the presence of non-white, sensor or external noise. This necessitates an estimation to be made of the noise statistics. Therefore, the ARMAX model structure:

$$\begin{aligned} y(t) + a_1 y(t-1) + \cdots + a_{n_a} y(t-n_a) \\ = b_1 u(t-1) + \cdots + b_{n_b} u(t-n_b) \\ + e(t) + c_1 e(t-1) + \cdots + c_{n_c} e(t-n_c) \end{aligned} \tag{2}$$

was selected for further analysis, where a_i, b_i and c_i are the parameters to be identified and $e(t)$ is a zero mean white noise. This structure takes into account both the true system and noise models.

The predictor for equation (2) is given by

$$\hat{y}(t\,|\,\theta) = \frac{B(q)}{C(q)} u(t) + \left[1 - \frac{A(q)}{C(q)}\right] y(t) \tag{3}$$

where

$\hat{y}(t\,|\,\theta)$ = predicted output according to model parameter θ

$$A(q) = 1 + a_1 q^{-1} + \cdots + a_{n_a} q^{-n_a}$$

$$B(q) = b_1 q^{-1} + \cdots + b_{n_b} q^{-n_b}$$

$$C(q) = 1 + c_1 q^{-1} + \cdots + c_{n_c} q^{-n_c}$$

This means that the prediction is obtained by filtering u and y through a filter with denominator dynamics determined by $C(q)$ [**17**].

The predictor (3) can be rewritten as

$$C(q)\hat{y}(t\,|\,\theta) = B(q)u(t) + [C(q) - A(q)]y(t) \tag{3a}$$

Adding $[1 - C(q)]\hat{y}(t\,|\,\theta)$ to both sides of equation (3a) gives

$$\begin{aligned} \hat{y}(t\,|\,\theta) = B(q)u(t) + [C(q) - A(q)y(t)] \\ + [1 - C(q)]\hat{y}(t\,|\,\theta) \end{aligned} \tag{3b}$$

Further, adding and subtracting $y(t)$ from the right-hand side of equation (3b) and collecting like terms together yields

$$\begin{aligned} \hat{y}(t\,|\,\theta) = B(q)u(t) + [1 - A(q)]y(t) \\ + [C(q) - 1][y(t) - \hat{y}(t\,|\,\theta)] \end{aligned} \tag{4}$$

Introducing the prediction error

$$\varepsilon(t, \theta) = y(t) - \hat{y}(t\,|\,\theta) \tag{5}$$

and the vector

$$\begin{aligned} \varphi(t, \theta) = [-y(t-1) \cdots -y(t-n_a) \\ u(t-1) \cdots - u(t-n_b) \\ \varepsilon(t-1, \theta) \cdots \varepsilon(t-n_c, \theta)]^{\mathrm{T}} \end{aligned} \tag{6}$$

equation (4) can be expressed as

$$\hat{y}(t\,|\,\theta) = \varphi^{\mathrm{T}}(t, \theta)\theta \tag{7}$$

where now

$$\theta = [a_1 \cdots a_{n_a} \;\; b_1 \cdots b_{n_b} \;\; c_1 \cdots c_{n_c}]$$

Equation (7) is referred to as a pseudo-linear regression due to the non-linear effect of θ in the vector $\varphi(t, \theta)$.

In the time-domain identification, prediction errors or residuals $\varepsilon(t)$ are analysed for arriving at an appropriate model structure. Residuals are the errors observed between the model response and the actual response of the plant to the same excitation. A model structure can be found, iteratively, that minimizes the absolute sum of the residuals. Ideally, the residuals $\varepsilon(t)$ should be reduced to an uncorrelated sequence denoted by $e(t)$ with zero mean and finite variance. Correlation-based model validity tests are employed to verify whether

$$e(t) \approx \varepsilon(t) \tag{8}$$

This can be achieved by verifying whether all the correlation functions are within the confidence intervals. When equation (8) is true, then

$$\varphi_{\varepsilon\varepsilon}(\tau) = E[\varepsilon(t-\tau)\varepsilon(t)] = \delta(\tau) \tag{9a}$$

$$\varphi_{u\varepsilon}(\tau) = E[u(t-\tau)\varepsilon(t)] = 0 \qquad \forall\tau \tag{9b}$$

where E is the expected or mean value. The quantities

$\phi_{\varepsilon\varepsilon}(\tau)$ and $\phi_{u\varepsilon}(\tau)$ are the estimated autocorrelation function of the residuals and the cross-correlation function between $u(t)$ and $\varepsilon(t)$ respectively; $\delta(\tau)$ is an impulse function. These two tests can be used to check the deficiencies of both the plant and the noise models. The expression in equation (9b) implies that the plant model is correct and the residuals are uncorrelated with the input. However, if $\phi_{\varepsilon\varepsilon}(\tau) \neq \delta(\tau)$, then it is an indication that although the plant model is correct, the noise model is incorrect and therefore the residuals are autocorrelated. On the other hand, if the noise model is correct and the plant model is biased, then the residuals are both autocorrelated such that $\phi_{\varepsilon\varepsilon}(\tau) \neq \delta(\tau)$ correlated with the input $\phi_{u\varepsilon}(\tau) \neq 0$.

5.3 Identification

Having selected a model structure, it is next desired to estimate the parameter vector θ. The search for the best model within the set then becomes a problem of determining or estimating θ. Once the model and the predictor are given, the prediction errors are computed as in equation (5). The parameter estimate $\hat{\theta}_N$ is then chosen to make the prediction error $\varepsilon(1, \theta), \ldots, \varepsilon(N, \theta)$ small. One of the common methods used to obtain $\hat{\theta}_N$ is to minimize a quadratic cost function $V_N(\theta)$, defined as

$$V_N(\theta) = \frac{1}{2} \sum_{t=1}^{N} \varepsilon^2(t, \theta) \tag{10}$$

where N denotes the number of data points. This problem is known as the 'non-linear least-squares problem' in numerical analysis. However, since $\hat{y}(t\,|\,\theta)$ in equation (7) is a non-linear function of θ, therefore the function $V_N(\theta)$ cannot be minimized analytically. Instead, some numerical minimization routines, such as the gradient or steepest-descent and Gauss–Newton, can be used to determine $\hat{\theta}_N$. This approach to estimation of the parameter vector $\hat{\theta}_N$ is referred to as the prediction error method (PEM). Thus, the system identification process using the PEM can be summarized as follows:

1. Choose a model structure (model type and order) and a predictor of the form in equations (2) and (3) respectively.
2. Select a cost function [equation (10)].
3. Form an initial estimate of $\hat{\theta}_N^{(1)}$ by a procedure outlined in reference [**20**]. The recommended approach leads to faster convergence of $\hat{\theta}_N$ and, therefore a shorter computing time.
4. Minimize $V_N(\theta)$ iteratively by one of the numerical methods, e.g. Gauss–Newton, until $\hat{\theta}_N$ converges.
5. Substitute $\hat{\theta}_N$ in equation (3) and find the prediction errors $\varepsilon(t, \theta)$.
6. Carry out the residual tests of equation (9). If satisfactory go to model validation (section 5.4). If not, change the model order and go to step 3, and then iterate until equations (9a) and (9b) are satisfied.

The PRBS signal was used for excitation and a multistep input (3211) and a doublet were used for cross-validation. These signals along with their corresponding outputs are shown in Figs 8, 9 and 10 respectively. Initially a second-order ARMAX model with 9 time delay terms was investigated. This satisfied the residual tests criterion as well as describing the dynamics reasonably well. However, a fourth-order model was employed, which gave better representation of system dynamics than the second-order model. The fourth-order model response can be seen in Fig. 11. These results are discussed in more detail in the next section. Hence,

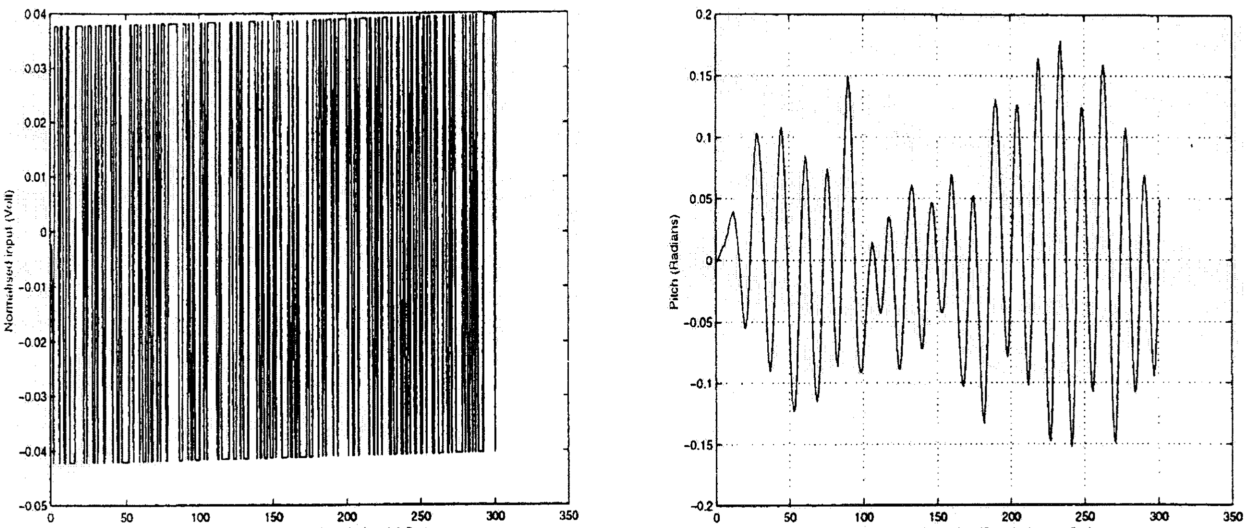

(a) PRBS input for system identification

(b) System response to a PRBS input

Fig. 8 Input and output signals used for modelling

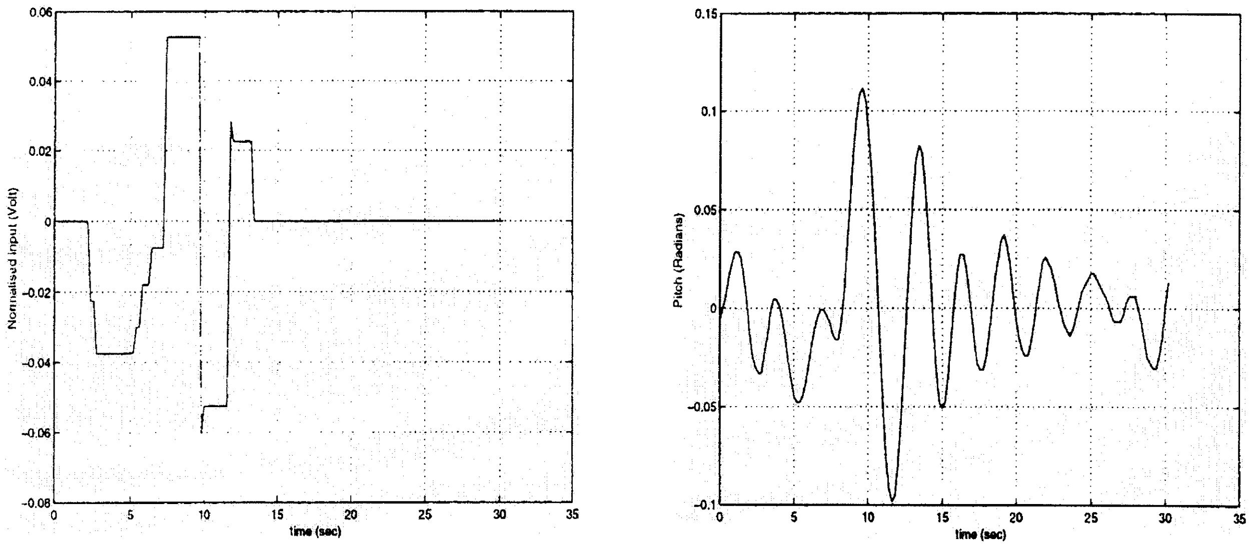

(a) Multi-step input (3211)

(b) System response to a multi-step input

Fig. 9 Input and output signals used for model cross-validation

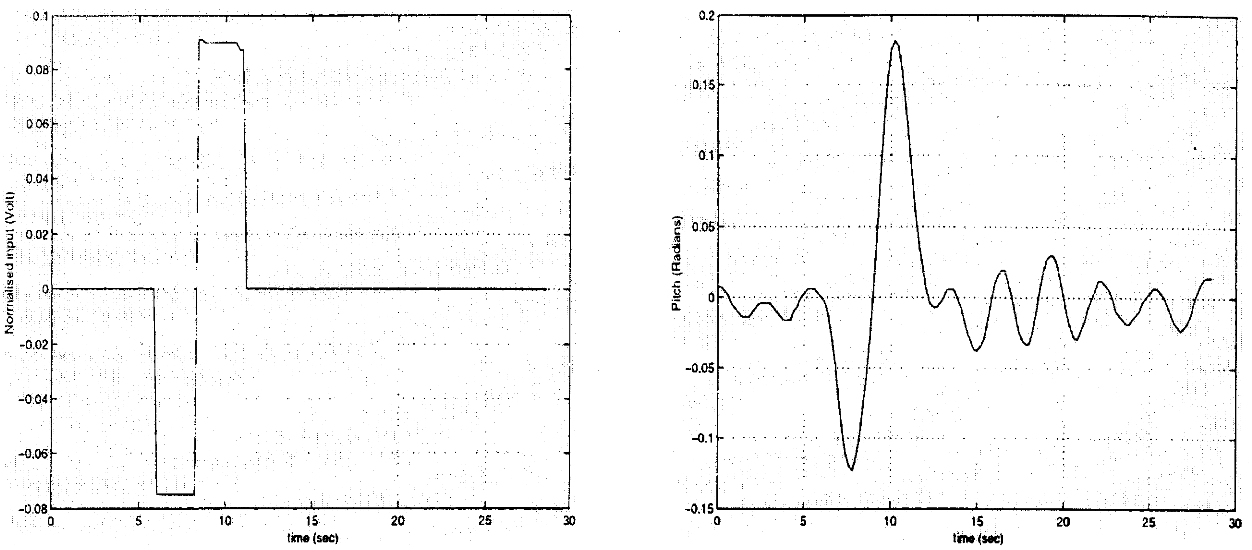

(a) Doublet input

(b) System response to a doublet

Fig. 10 Input and output signals used for model cross-validation

subsequent investigations are based on the fourth-order ARMAX model, using the MATLAB system identification toolbox [**20**]. The toolbox utilizes the PEM to estimate the model parameters and incorporates the IV method for an initial estimate of $\hat{\theta}_N^{(1)}$.

Figure 12a depicts the autocorrelation test of residuals, signifying that the noise has been modelled adequately and also that the model order is appropriate. The cross-correlation function between the residuals and the input is shown in Fig. 12b, which is well within the 95 per cent confidence band, marked by the dotted lines. Independence between residuals and inputs is imperative, which is a measure of a proper estimation of time delays.

The Bode plots of the model are shown in Fig. 13. Both the gain and phase plots of the estimated model are in good agreement with the gain and phase obtained from the actual system response. This model gives a reliable representation of the TRMS dynamics and, as will be shown next, has a high predictive capability.

5.4 Time-domain validation

Verification is a key final step in a system identification process, which assesses the predictive quality of the extracted model. Data not used in the estimation are selected in order to ensure that the model is not tuned to specific data records or input forms. Major deficiencies in the model structure and parameter estimates

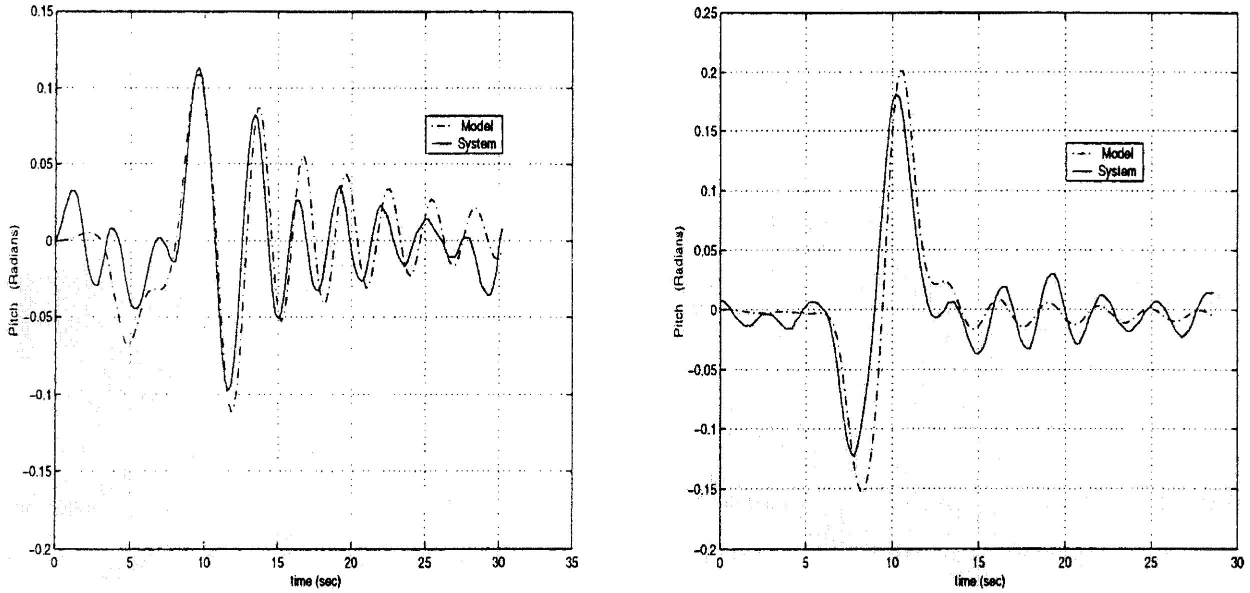

(a) With a 3211 input

(b) With a doublet input

Fig. 11 The system and model response

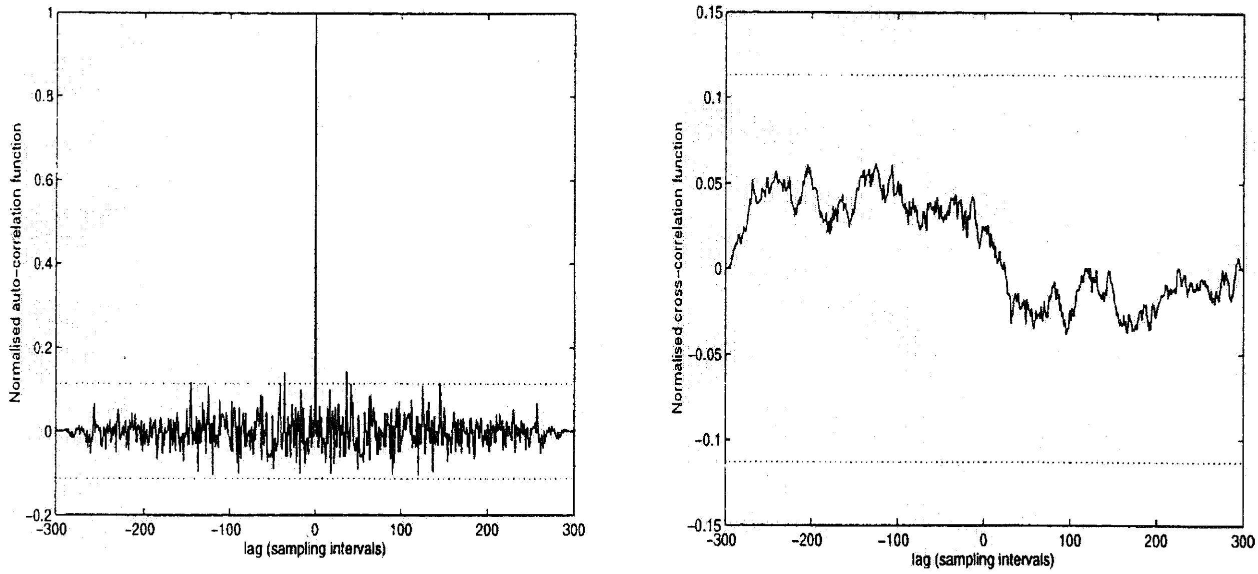

(a) Auto-correlation of residuals

(b) Cross-correlation of input and residuals

Fig. 12 Residual test

would give rise to obvious errors in the model output sequence. The excitation signal used in the comparison could be the same as was used to identify the model. In practice, it is desirable to obtain further plant responses to an excitation signal that has slightly different frequency components. In this cross-validation study, the model is tested against two different sets of input records: (a) multi-step input and (b) doublet. In Fig. 11 the simulated model output and the experimental outputs are compared. Figure 11a depicts the responses for a multi-step input and Fig. 11b for a doublet. The identified model appears capable of simulating the manoeuvring behaviour of the TRMS with reasonable accuracy, as the model closely follows the actual system output. Overall, the predictive capability of the model is quite good, especially considering the sensitive nature of the TRMS to ambient disturbances. Although there are still some discrepancies, the overall agreement is satisfactory. These discrepancies can be attributed to (a) a non-linear regime at 0.4 Hz frequency, (b) a mild oscillatory nature of the TRMS, even in the steady state, as well as being (c) very sensitive to the slightest atmospheric disturb-

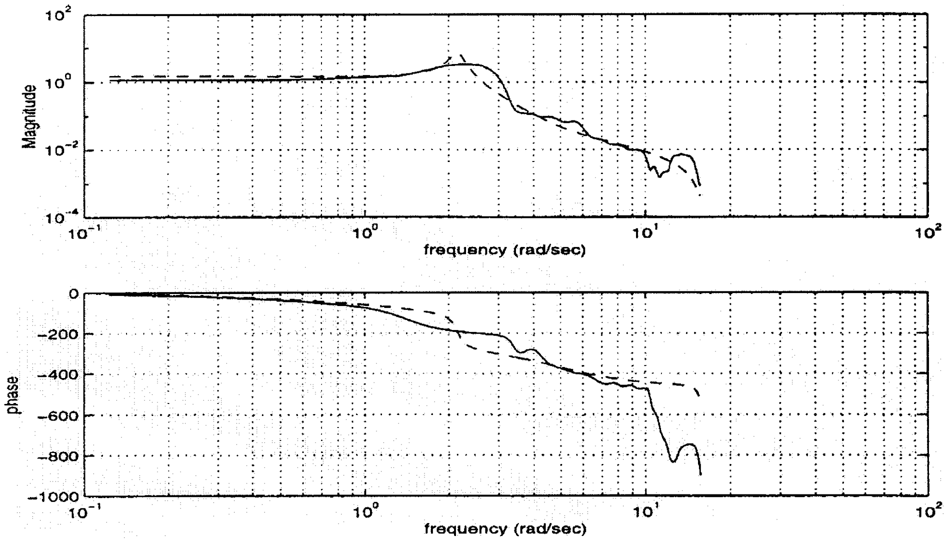

Fig. 13 Bode plot

ance. The combined effect is reflected in these figures with the occasional shooting of peaks due to a slight wind, even when the input signals have ceased to exist.

A few differences are worth noting. On the whole, the faster dynamics of the model do correspond well with the system results but the slower more dominant dynamics do not respond very well. However, it is presumed that the resulting model is suitable for further control analysis.

5.5 Frequency domain validation

In frequency domain cross-validation tests, emphasis is placed on the ability of the model to predict system modes. Power spectral density plots of the plant and model outputs are superimposed and compared in Fig. 14. It is noted that the dominant modes of the model and the plant coincide with one another quite well, implying a good model predicting capability of the important system dynamics. Thus, from the foregoing analysis it can be concluded that the model has captured the important plant dynamics quite well.

5.6 Transparent black-box model and interpreting the black-box model

In this work, the black-box approach is adopted in order to circumvent the tedious mathematical modelling process. However, it may be desirable to give physical meaning to the model coefficients and undertstand their influence on the vehicle motion. Such an understanding would aid system analysis, controller design and even redesigning or modifying the vehicle component(s) to achieve the desired system dynamic characteristics. Therefore, in this section an attempt is made to interpret the extracted black-box model, i.e. to relate the

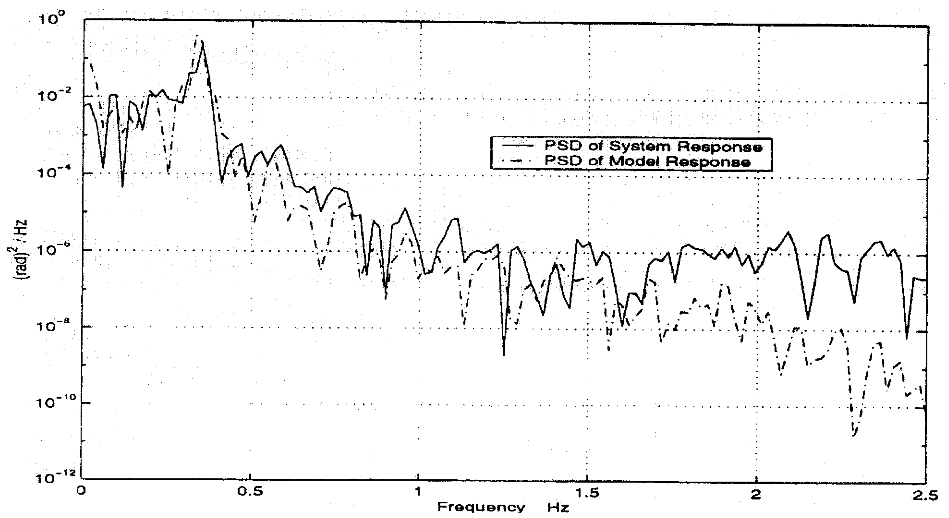

Fig. 14 Frequency domain validation

parameters of the model to the actual system dynamic behaviour. If there is interest only in an input–output representation of the pitch axis of the TRMS, a discrete-time transfer function can be obtained from the identified parametric model:

$$\frac{y(z)}{u(z)} = \frac{0.0097z^3 - 0.0086z^2 + 0.006z + 0.0284}{z^4 - 3.0077z^3 + 3.5001z^2 - 1.8096z + 0.3407} \tag{11}$$

where

y = pitch angle (rad)
u = main rotor input (V)

The coefficients of the transfer function in equation (11) have no physical meaning, but the dynamic characteristics of the system depend directly upon them, and it would be interesting to make it evident in the structure. Factoring the numerator and the denominator polynomials of equation (11) yields

$$\frac{y(z)}{u(z)} = \frac{(z - 0.9805 + 1.3281\mathrm{i}) \times (z - 0.9805 - 1.3281\mathrm{i})(z + 1.0743)}{(z - 0.8926 - 0.4095\mathrm{i})(z - 0.8926 + 0.4095\mathrm{i}) \times (z - 0.7541)(z - 0.4685)} \tag{12}$$

implying that the system has complex poles, thus bringing into evidence the (almost) unstable oscillatory mode, which is a significant dynamic characteristic of the TRMS and also of a helicopter in hover. The oscillatory or vibrationtal motion is imparted to the system due to flexible structural component(s). The complex poles in the characteristic equation are therefore directly related to the physical properties of the structural material. This is further discussed in the next section.

For a 1 DOF purely rigid body, it takes two state variables (one position and one velocity) to describe the motion of the body. Thus, the real poles in equation (12) represent two state variables, which describe the rigid-body motion, namely pitch angle and pitch velocity. Note that the system is non-minimum phase, with zeros outside the unit circle. Interpretation of the black-box model thus brings to the fore similar information to that obtained from the mathematical modelling process.

6 VIBRATION CONTROL OF THE TRMS

In general, for flexible structures/aircraft, the parameter that has an influence on the flexible modes is the mass distribution, which may change the frequencies of the modes and the accuracy of the model. In the case of aircraft, the speed and Mach number also have an influence on the modes of the system. This is relevant to the TRMS, which can be interpreted as a centrally supported cantilever beam with loads (rotors) at both ends. The non-uniform mass distribution due to the rotors and the rotor torque at normal operating conditions are the main causes of beam deflection. The deflection of the beam is due to the excitation of the resonance modes by an input signal that is rich in the system's eigenfrequencies. The different deflection profiles of the beam, occurring at corresponding resonance frequencies, represent the system's normal mode shape. Thus, in theory, the beam will have an infinite number of such normal modes with associated mode shapes and frequencies.

Conventionally, a dynamic system is excited by a fluctuating force, the frequency of which is equal to the natural frequency of the dynamic system. The TRMS could oscillate and become unstable if its natural frequency of oscillation is of the same order or is close or within the frequency range of the disturbance/excitation due to the rotor. Hence, accurate identification and subsequent processing of these modes is important from a systems engineering perspective. In particular, this is important for designing control laws to ensure that structural component limits and fatigue loads are not exceeded for the full operating range of aircraft/TRMS manoeuvres. Moreover, this will be useful for minimizing structural damage via suppression of vibration at resonance modes, reduction in pilot workload and passenger comfort in the case of an aircraft.

The presence of the main resonance mode at 0.34 Hz, evident from the results in Section 5.1, is the primary cause of residual vibration in the TRMS. The residual motion (vibration) is induced in flexible structures primarily as a result of faster motion commands. The occurrence of any vibration after the commanded position has been reached will require additional settling time before the new manoeuvre can be initiated. Therefore, in order to achieve a fast system response to command input signals, it is imperative that this vibration is reduced. This feature is desirable in fast manoeuvring systems, such as fighter aircraft. Various approaches have been proposed to reduce vibration in flexible systems. They can be broadly categorized as feedforward, feedback or a combination of feedforward and feedback methods.

Feedback control approaches utilize measurements and estimates of the system states to reduce vibration. However, fast tracking performance is always constrained by the physical limit of the actuator rate. A common practice in coping with this dilemma is to use an actuator rate limiter. A major drawback of this method is that the system becomes unpredictable when the actuator rate is saturated. This may result in limit cycles or even instability.

An alternative approach is to use a feedforward filter, which alters the tracking command or setpoints so that system oscillations are reduced. The performance of feedback methods can often be improved by additionally using a feedforward controller and suitably designed feedforward compensators can significantly reduce the complexity of the required feedback controllers for a given level of performance. The current study will be confined to the design and implementation of a digital feedforward filter for command shaping and leave the combined controller for future investigation.

Open-loop control methods have been considered in vibration control where the control input is developed by considering the physical and vibrational properties of the flexible system. The goal of this research is to develop methods to reduce motion and uneven mass-induced vibrations in the TRMS during operation. The assumption is that the motion and the rotor load are the main sources of system vibration. Thus, input profiles, which do not contain energy at system natural frequencies, do not excite structural vibration and hence require no additional settling time. Digital filters are used for preprocessing the input to the plant, so that no energy is ever put into the system near its resonances. The filter design process can be found in most standard texts [**21**].

To study the system performance initially an unshaped doublet input is used and the corresponding system response is measured. The main objective of this section is to suppress the system vibrations at the first few dominant resonance modes.

6.1 Low-pass filter shaped input

A low-pass Butterworth filter of order three with a cut-off frequency at 0.1 Hz was designed and employed for off-line processing the doublet input. The motive behind selecting the cut-off frequency at 0.1 Hz lies in the fact that the lowest vibrational mode of the system is found to be at 0.25 Hz. Hence, to attenuate resonance of the system the cut-off frequency must be selected lower than the lowest vibrational mode. The shaped doublet input is then injected to the TRMS and the pitch response is measured. The low-pass Butterworth filtered doublet is shown in Fig. 15 and the corresponding pitch response in Fig. 16. It is noted that the attenuation in the level of vibration at the first and second resonance modes of the system are 5.83 and 7 dB respectively (see Fig. 16), with the shaped input in comparison to the unshaped doublet.

6.2 Band-stop filter shaped input

As above, a third-order digital Butterworth filter is used to study the TRMS performance with a band-stop shaped input. For effective suppression of the vibrations of the system, the centre frequency of the band-stop filter has to be exactly at the same frequency or closer to the resonance modes. As noted in Fig. 3b and Section 4.1, the main resonant mode lies at 0.34 Hz, with additional clustered modes in close proximity to the main mode. Thus, a band-stop frequency range of 0.2–0.4 Hz was selected for the filter design. A band-stop shaped doublet input was accordingly used and the pitch response was measured. The shaped doublet input and the corresponding system response are shown in Figs 17 and 18 respectively. It is noted that the spectral attenuation in the level of system vibration at the first and second modes were 0.83 and 1.8 dB respectively.

7 CONCLUSION

A 1 DOF SISO TRMS model, whose dynamics have some features in common with those of a helicopter, has been successfully identified. Both time- and frequency-domain analyses were utilized to investigate and develop confidence in the obtained model. The extracted model has predicted the system behaviour well. An attempt was also made to relate the black-box model parameters to the actual plant dynamics, thus bringing into evidence the marginally stable oscillatory mode, which is a significant dynamic characteristic of the TRMS. Some aspects of the modelling approach presented may be relevant for flight mechanics modelling of new generations of air vehicle.

Modelling of the TRMS revealed the presence of resonant modes, which are responsible for inducing unwanted vibrations. The extracted model has been employed for designing and implementing feedforward/open-loop control. In these methodologies, a feedforward input signal is shaped so that it does not contain spectral components at the system's resonance eigenfrequencies. The study revealed that a better performance in attenuation of system vibration at the resonance modes is achieved with the low-pass filtered input, as compared to the band-stop filter. This is due to indiscriminate spectral attenuation at frequencies above the cut-off level in the low-pass filtered input. However, this is at the expense of a slightly higher move time as compared to the band-stop filter. The modelling and control approach presented is quite suitable for modern flexible plants with complex dynamics.

ACKNOWLEDGEMENTS

S. M. Ahmad gratefully acknowledges the financial support of the University of Sheffield and the Department of Automatic Control and Systems Engineering during the course of this project. The authors would also like to thank Dr H. A. Thompson, Manager, Rolls–Royce University Technology Centre in Control and Systems Engineering, the University of Sheffield, for many valuable comments on helicopter dynamics and for reviewing the manuscript.

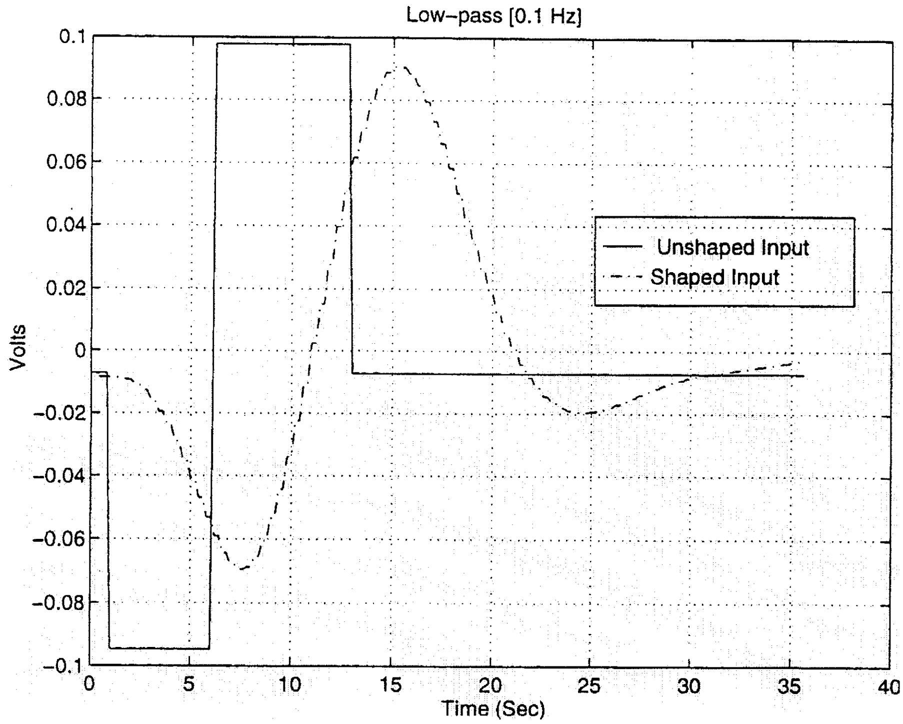

(a) Time domain

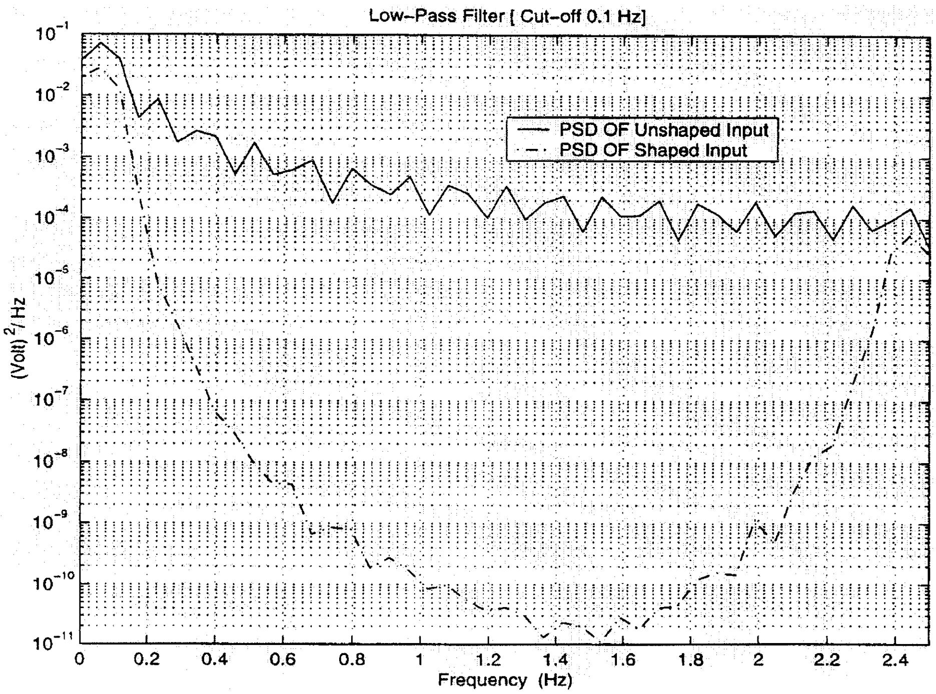

(b) Power spectral density

Fig. 15 Doublet input using a third-order Butterworth low-pass filter

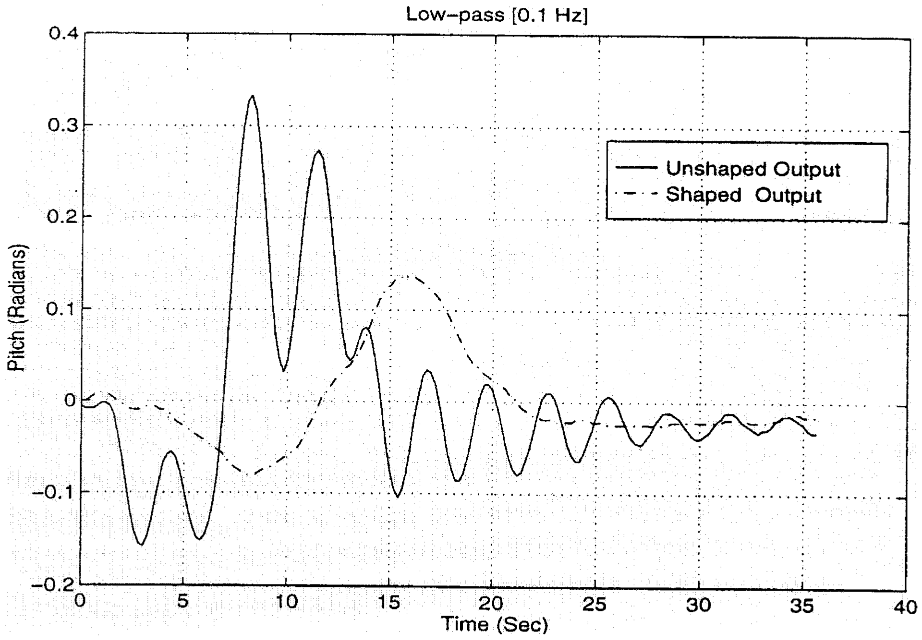

(a) Time domain

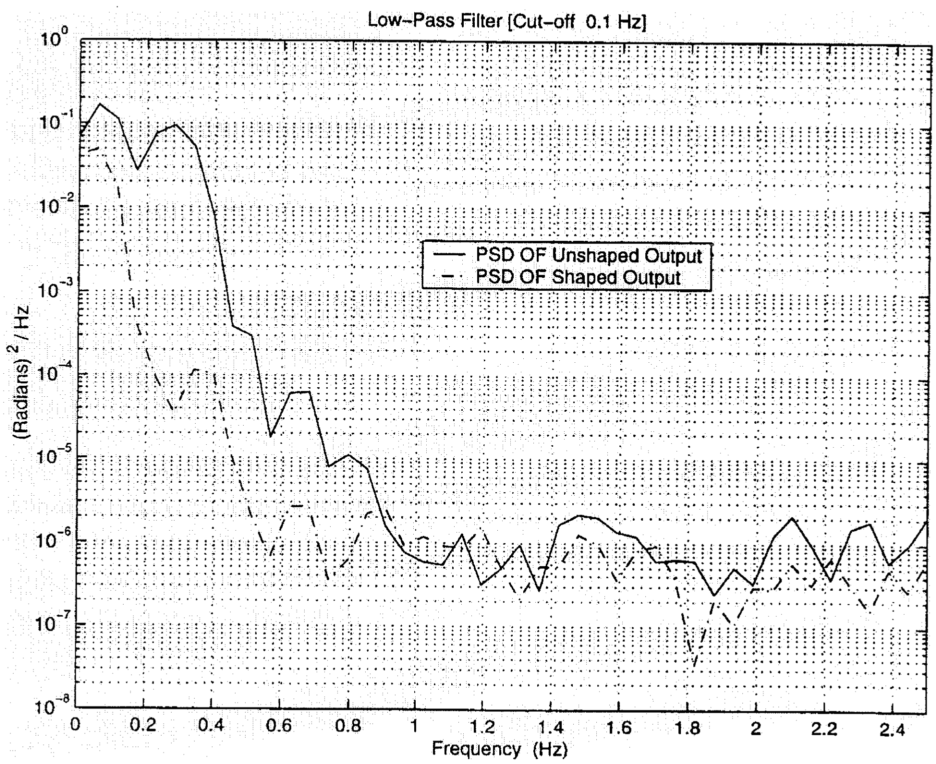

(b) Power spectral density

Fig. 16 Pitch response with a third-order Butterworth low-pass filtered doublet input

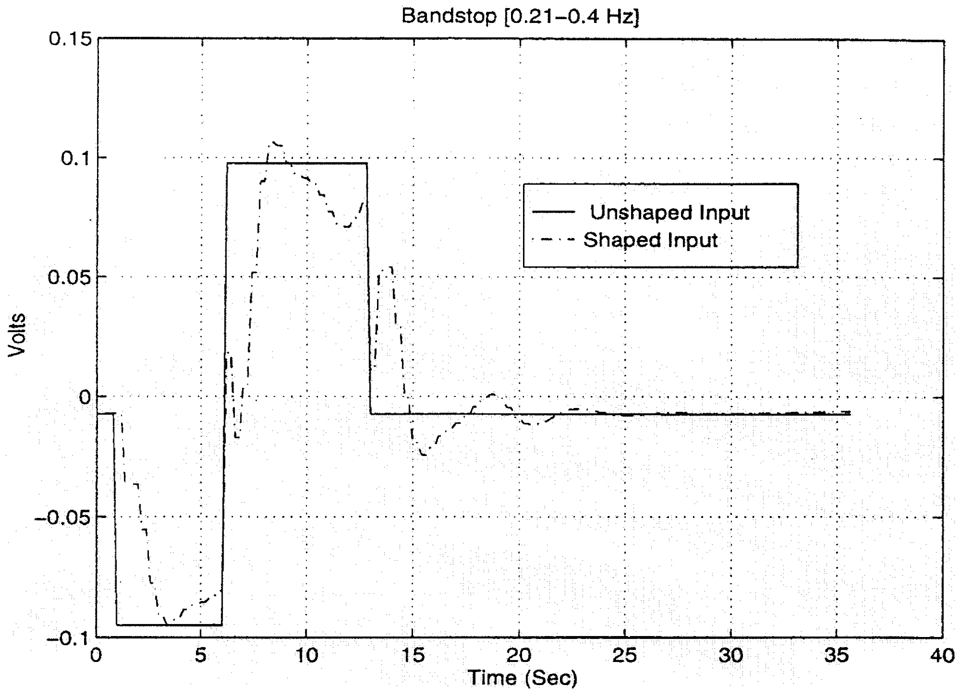

(a) Time domain

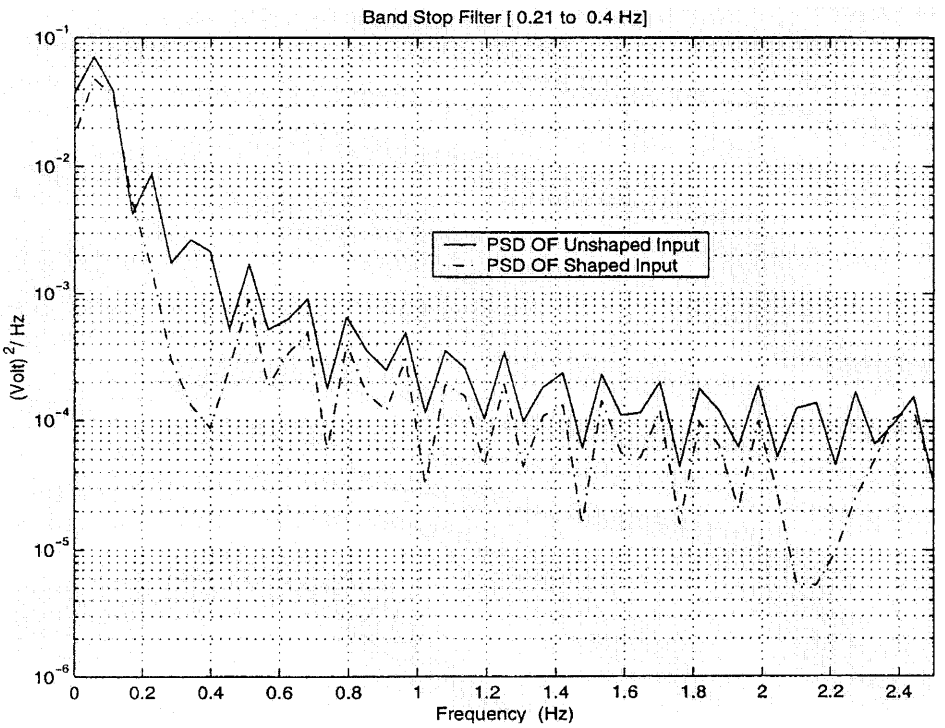

(b) Power spectral density

Fig. 17 Doublet input using a third-order Butterworth band-stop filter

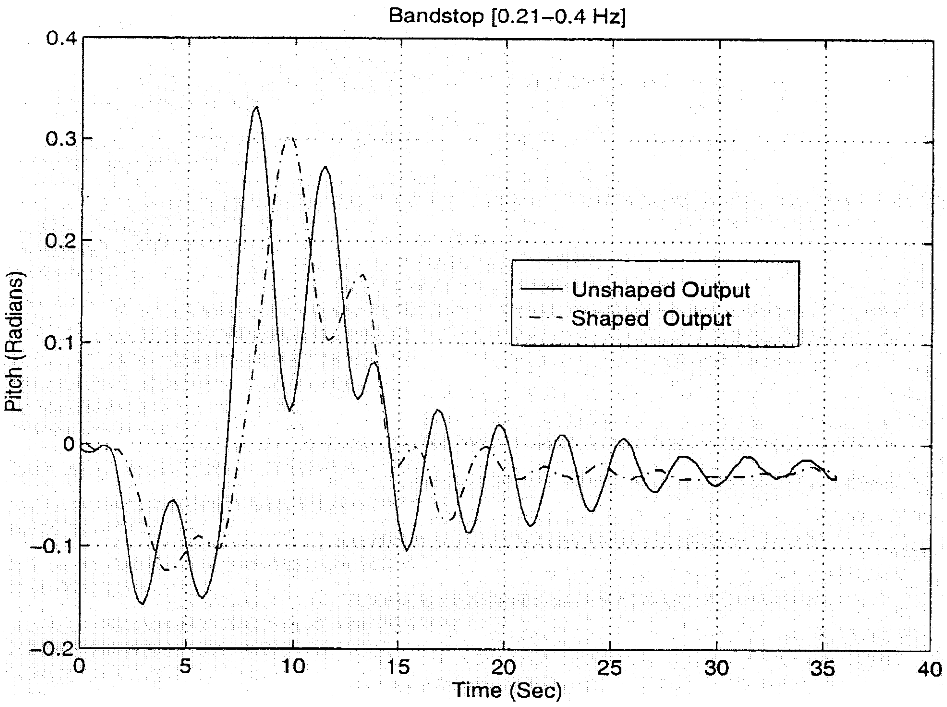

(a) Time domain

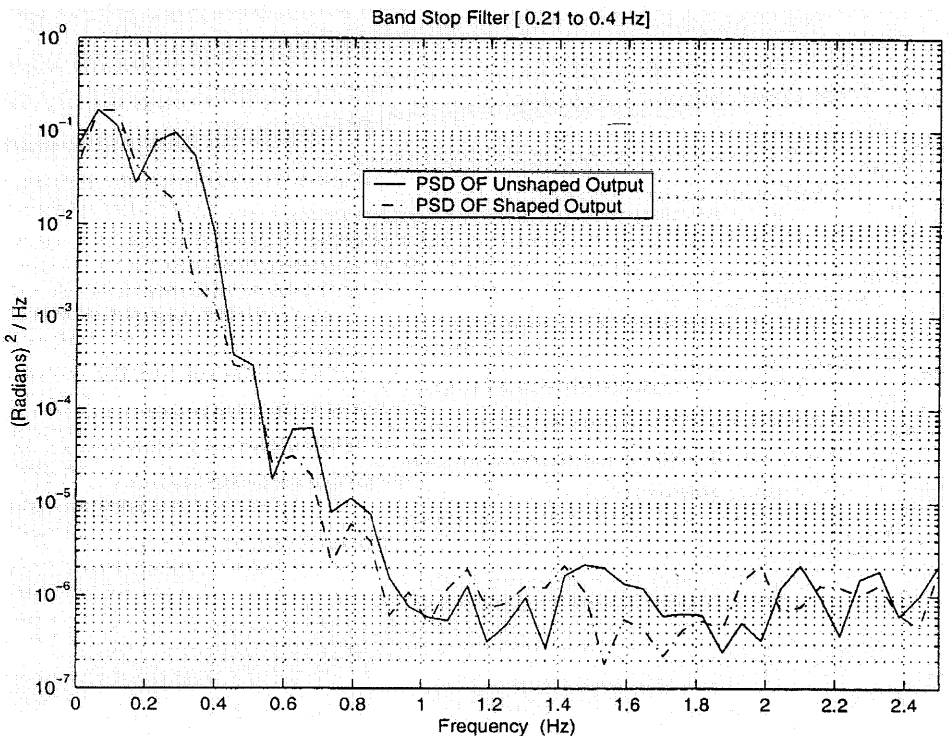

(b) Power spectral density

Fig. 18 Pitch response with the Butterworth band-stop filtered doublet input

REFERENCES

1 **Livet, T., Fath, D.** and **Kubica, F.** Robust autopilot design for a highly flexible aircraft. In Proceedings of IFAC World Congress, San Francisco, California, July 1996, pp. 279–284.

2 **George, K. K.** and **Bhat, M. S.** Two-degree-of-freedom $H_{-\infty}$ robust controller for a flexible missile. *J. Guidance, Control, and Dynamics*, 1998, **21**, 518–520.

3 **Turnour, S. R.** and **Celi, R.** Modelling of flexible rotor blades for helicopter flight dynamics applications. *J. Am. Helicopter Soc.*, 1996, **41**, 52–66.

4 **Waszak, M. R.** and **Schmidt, D. K.** Flight dynamics and aeroelastic vehicles. *J. Aircr.*, 1988, **25**, 263–271.

5 **Waszak, M. R.** and **Schmidt, D. K.** Modelling and model simplification of aeroelastic vehicles: an overview. NASA Technical Memorandum 107691, 1992.

6 *Methods for Aircraft State and Parameter Identification*, 1974 (AGARD, NASA Research Centre, Hampton, Virginia).

7 **Bruce, P. D., Silva, J. E.** and **Kellet, F. M. G.** Maximum likelihood identification of linear aircraft dynamics using a hybrid genetic algorithm. In Proceedings of AIAA 36th Aerospace Sciences Conference, Reno, Nevada, 1998.

8 **Tischler, M. B.** System identification methods for aircraft flight control development and validation. In *Advances in Aircraft Flight Control* (Ed. M. B. Tischler), 1996, pp. 35–69 (Taylor and Francis, London).

9 **Kaletka, J., Tischler, M. B., von Grunhagen, W.** and **Fletcher, J. W.** Time and frequency-domain identification and verification of BO 105 dynamic models. *J. Am. Helicopter Soc.*, 1991, 25–38.

10 **Mettler, B., Kanade, T.** and **Tischler, M. B.** System identification modelling of a model-scale helicopter. Technical Report CMU-RI-TR-00-03, Robotics Institute, Carnegie-Mellon University, Pittsburgh, Pennsylvania, 2000.

11 **Ahmad, S. M., Chipperfield, A. J.** and **Tokhi, M. O.** Modelling and control of a twin rotor multi-input multi-output system. In Proceedings of the American Control Conference, Chicago, Illinois, June 2000, pp. 1720–1724.

12 **Ahmad, S. M., Chipperfield, A. J.** and **Tokhi, M. O.** Parametric modelling and dynamic characterization of a two-degree-of-freedom twin rotor multi-input multi-ouput system. *Proc. Instn Mech. Engrs, Part G, Journal of Aerospace Engineering*, 2001, **215**(G2), 63–78.

13 **Landis, H. K., Davis, J. M., Dabundo, C.** and **Keller, J. F.** Advanced flight control research and development at Boeing Helicopter. In *Advances in Aircraft Flight Control* (Ed. M. B. Tischler), 1996, pp. 103–141 (Taylor and Francis, London).

14 *Twin Rotor MIMO System*, Manual 33-007-0, 1996 (Feedback Instruments Limited, Sussex).

15 **Ljung, L.** *System Identification: Theory for the User*, 1999, 2nd edition (Prentice-Hall, Englewood Cliffs, New Jersey).

16 **Wellstead, P. E.** and **Zarrop, M. B.** *Self-Tuning Systems: Control and Signal Processing*, 1991 (John Wiley, Chichester, West Sussex).

17 **Soderstrom, T.** and **Stoica, P.** *System Identification*, 1989 (Prentice-Hall, Englewood Cliffs, New Jersey).

18 **Bendat, J. S.** and **Piersol, A. G.** *Engineering Application of Correlation and Spectral Analysis*, 1980 (John Wiley, Chichester, West Sussex).

19 **Patton, R., Miles, M.** and **Taylor, P.** Design and application of test signals for helicopter model validation in the frequency domain. In *Perturbation Signals for System Identification* (Ed. W. Godfrey), 1993, pp. 298–320 (Prentice-Hall, Englewood Cliffs, New Jersey).

20 **Ljung, L.** *System Identification Toolbox*, 1991 (MathWorks Inc., Natick, Massachusetts).

21 **Oppenheim, A. V.** and **Schafer, R. W.** *Discrete-Time Signal Processing*, 1999 (Prentice-Hall, Englewood Cliffs, New Jersey).